Wave-Mixing and Vector Phase Conjugation by Polarization-Dependent Saturable Absorption in Cr^{4+}:YAG

M. J. Damzen,* S. Camacho-Lopez, and R. P. M. Green
The Blackett Laboratory, Imperial College, London SW7 2BZ, United Kingdom
(Received 6 February 1996)

We describe a theory of four-wave mixing in the saturable absorber Cr^{4+}:YAG and compare with experiments performed at 1.064 μm wavelength. We show that the strong polarization dependence of the saturable absorption along orthogonal crystallographic axes leads to unique polarization properties for wave mixing in Cr^{4+}:YAG. Also there are a range of conditions that lead to vector phase conjugation of the polarization state of a signal beam. Optimum reflectivity for vector phase conjugation occurs when the pump beams have either orthogonal circular polarizations or parallel linear polarizations at 45° to the crystallographic axes. The latter case is unique to this type of nonlinearity.

PACS numbers: 42.65.Hw, 42.40.Eq, 42.81.Gs

There have been numerous studies performed on nonlinear optics in saturable media and particularly in induced population grating studies for beam diffraction and phase conjugation in saturable amplifiers [1,2] and saturable absorbers [3]. Very high efficiency has been demonstrated in laser amplifiers [4]. Saturable absorbers generally have lower efficiency but offer greater simplicity, since the material is passive and does not require an inverting process. The material Cr^{4+}:YAG (denoted as Cr:YAG in this paper) is of considerable interest as a solid-state saturable absorber, particularly for its use in Q switching of Nd:YAG laser systems at wavelength (1.064 μm) [5–7]. Recent experiments on its saturable absorption and lasing properties indicate that Cr:YAG has strongly polarized species of the chromium ions [8] along orthogonal cyrstallographic axes. Optical radiation can only effectively access a subset of available Cr species whose dipole moment for transition from the ground state to the excited state is parallel to the optical polarization component. As a result, Cr:YAG must be considered as an inhomogeneous saturable absorber with respect to the polarization state of incident light. Greater saturation of one axis relative to another leads to an induced absorption birefringence and, therefore, under saturation conditions, input light polarization needs to be resolved along the crystallographic axes. We show in this paper that this leads to unique nonlinear wave-mixing behavior and, in particular, assess the suitability of Cr:YAG as a nonlinear medium to perform vector phase conjugation [9–12] of both the polarization and spatial state of an optical beam.

Initially, we perform a theoretical analysis of four-wave mixing in a polarization-dependent saturable absorber with characteristics corresponding to Cr:YAG. The results would also be valid for a corresponding polarization-dependent saturable amplifier. Theoretical predictions are compared to experimental results of four-wave mixing (FWM) in a Cr:YAG crystal performed by radiation from a pulsed Nd:YAG laser system. We investigate particularly the case when the counterpropagating pump beams have polarization states leading to vectorial phase conjugation (VPC) [12] of an arbitrary polarized, or depolarized, signal beam. Such a case is of particular interest for applications involving depolarization of laser radiation in solid-state laser systems, since a vector phase conjugate reflection can correct for combined phase and polarization aberrations that occur in solid-state amplifiers operating at high-average powers. We show that in this crystal there are combinations of pump polarizations that lead to VPC that do not occur in normal nonlinear media based on third-order susceptibilities or saturable media that are homogeneous to the polarization state. We demonstrate that VPC is, however, incomplete for a saturating signal beam.

Consider the case of Cr:YAG with a FWM interaction as shown in Fig. 1. We take the case (corresponding to our experiments that are described later) in which the beams propagate in directions approximately parallel or antiparallel to the surface normal which is along the crystallographic [100] axis denoted by direction vector **z**. Polarization vectors of the interacting beams are therefore transverse to this axis and lie in the x-y plane where the **x** axis is taken as parallel to the [010] crystallographic axis and the **y** axis parallel to the [001] axis.

The total atomic polarization amplitude due to the resonant absorbing species can be written in the form [13,14] $\mathbf{P}_T(r,t) = -i2\varepsilon_0\alpha/k\mathbf{E}(r,t)$ for an isotropic absorber,

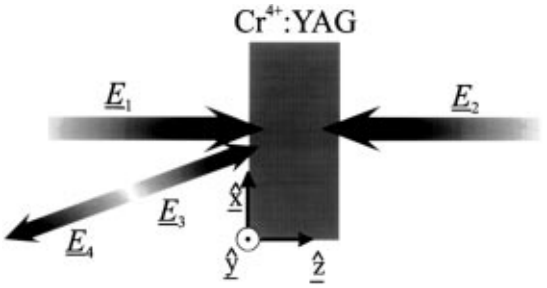

FIG. 1. Schematic diagram of four-wave mixing in Cr^{4+}:YAG showing three input beams $\mathbf{E}_1$–$\mathbf{E}_3$ of arbitrary polarization states and generated conjugate beam $\mathbf{E}_4$ and illustrating the orientation of the crystallographic axes as explained in the text.

 0031-9007/96/76(16)/2894(4)$10.00

where ε_0 is the permittivity of free space, $\alpha = \frac{1}{2}\sigma N$ is the (amplitude) absorption coefficient of the medium, σ is the cross section for absorption, N is the (saturable) number density of ground-state absorbing species, k is the magnitude of the optical wave vector, and $\mathbf{E}$ is the total optical field. In the case of Cr:YAG the absorbing species of Cr^{4+} are inhomogeneous with respect to polarization with polarization-sensitive species having number densities N_x, N_y, and N_z and giving rise to a tensorial absorption coefficient of the form $\boldsymbol{\alpha} = \alpha_x\mathbf{x} + \alpha_y\mathbf{y} + \alpha_z\mathbf{z} = \frac{1}{2}\sigma\,(N_x\mathbf{x} + N_y\mathbf{y} + N_z\mathbf{z})$ and such that, for field components E_x and E_y transverse to the z axis as shown in Fig. 1, the polarization is

$$\mathbf{P}_T = -i2\varepsilon_0/k[\alpha_x E_x\mathbf{x} + \alpha_y E_y\mathbf{y}]. \tag{1}$$

The components of the absorption coefficient themselves saturate with intensity, in the steady-state case, from a small-signal value α_0 according to

$$\alpha_{x,y} = \alpha_0/[1 + I_{x,y}/I_s], \tag{2}$$

where $I_{x,y}$ is the total intensity in the x and y polarization states, $I_s = h\nu/\sigma\tau$ is the saturation intensity of the medium, $h\nu$ is the photon energy, and τ is the upper-state lifetime. For simplicity, we take, initially, the case of weak saturation such that Eq. (2) can be approximated by $\alpha_{x,y} \approx \alpha_0(1 - I_{x,y}/I_s)$ and derive analytical solutions for the generation of the conjugate beam. Strong saturation effects by the pump and probe beams will be discussed later. The following analysis can also be adapted to the transient case by noting that under weak transient saturation conditions $\alpha_{x,y} = \alpha_0\exp(-U_{x,y}/U_s) \approx \alpha_0(1 - U_{x,y}/U_s)$ and has a similar form to the steady-state case but in terms of the optical fluence $U_{x,y}$ and saturation fluence of the medium $U_s = h\nu/\sigma$. For square pulses $[U(t) = It]$ the transient solution for the conjugate field $\mathbf{E}_4(t)$ is related to the steady-state value $\mathbf{E}_4^{ss}$ by the relation $\mathbf{E}_4(t) = \mathbf{E}_4^{ss}t/\tau$.

We write the fields in the form

$$\mathbf{E}_i(r) = \tfrac{1}{2}\,\mathbf{A}_i(z)\exp[i(\omega t - \mathbf{k}_i\cdot\mathbf{z})] + \text{c.c.}, \tag{3a}$$

$$\mathbf{A}_i(z) = \begin{bmatrix} A_{ix}(z) \\ A_{iy}(z) \end{bmatrix}, \tag{3b}$$

where $\mathbf{k}_i = +|k|\mathbf{z}$ for forward propagating beams 1 and 3 and $\mathbf{k}_i = -|k|\mathbf{z}$ for backward propagating beams 2 and 4 and the field amplitudes $\mathbf{A}_i$ are resolved along the crystallographic axes. In the weak saturation approximation, we take pump and probe beams ($\mathbf{E}_1$, $\mathbf{E}_2$, and $\mathbf{E}_3$) to experience small-signal absorption and selecting phase-matched terms in the polarization that contribute to the conjugate beam $\mathbf{E}_4$ in Maxwell's wave equation. This results in the following set of equations for the field amplitudes:

$$A_1(z) = \exp(-\alpha_0 z)\begin{bmatrix} A_{1x}(0) \\ A_{1y}(0) \end{bmatrix}, \tag{4a}$$

$$A_2(z) = \exp[-\alpha_0(L - z)]\begin{bmatrix} A_{2x}(L) \\ A_{2y}(L) \end{bmatrix}, \tag{4b}$$

$$A_3(z) = \exp(-\alpha_0 z)\begin{bmatrix} A_{3x}(0) \\ A_{3y}(0) \end{bmatrix}, \tag{4c}$$

$$\frac{d}{dz}\begin{bmatrix} A_{4x}(z) \\ A_{4y}(z) \end{bmatrix} = +\alpha_0\begin{bmatrix} A_{4x}(z) \\ A_{4y}(z) \end{bmatrix} - \alpha_0\exp(-\alpha_0 z) \times \exp(-\alpha_0 L)\hat{M}\begin{bmatrix} A_{3x}^*(0) \\ A_{3y}^*(0) \end{bmatrix}, \tag{4d}$$

$$\hat{M} = \begin{bmatrix} 2A_{1x}(0)A_{2x}(L) & 0 \\ 0 & 2A_{1y}(0)A_{2y}(L) \end{bmatrix}, \tag{4e}$$

where L is the length of the crystal, M is a 2×2 transformation matrix, and (complex) field amplitudes are in normalized saturation intensity units with magnitude such that $|A| = \sqrt{I/I_s}$. With the boundary condition $\mathbf{A}_4(L) = 0$, solution of Eq. (4d) for the output conjugate field $\mathbf{A}_4(0)$ is given by

$$\begin{bmatrix} A_{4x}(0) \\ A_{4y}(0) \end{bmatrix} = \frac{1}{2}\exp(-\alpha_0 L) \times [1 - \exp(-2\alpha_0 L)]\hat{M}\begin{bmatrix} A_{3x}^*(0) \\ A_{3y}^*(0) \end{bmatrix}. \tag{5}$$

Equation (5) shows that beam 4 has the spatial form of the phase conjugate of beam 3 if $\mathbf{E}_3$ is a pure polarization state and if the pumps are plane waves (or spatial phase conjugates of each other). However, beam 4 is not generally the vectorial phase conjugate VPC of beam 3 unless the matrix M is proportional to the identity matrix [12]. It is interesting to note that due to the polarization inhomogeneity of the absorbing species there are no off-diagonal elements in matrix M and the conjugation of the x and y components of probe beam $\mathbf{A}^3$ occur independently with no admixture. This is a different characteristic from most other nonlinear media [12]. Some examples of the 2×2 transformation matrix M are listed in Table I for different pump polarization conditions, and it is noted that field components A_{1x}, A_{1y}, A_{2x}, and A_{2y} are complex amplitudes. Table I shows that pump beams with orthogonal circular polarizations produce a 2×2 identity matrix corresponding to the condition for vector phase conjugation VPC [12]. This is in correspondence to the general condition for VPC in many other nonlinear media. However, in Cr:YAG there is a larger range of cases that lead to VPC, and these occur when $A_{1x}, A_{2x} = A_{1y}A_{2y}$, in terms of the magnitude of both amplitudes and phases. Taking

$$A_1 = |A_1|\begin{bmatrix} \cos\theta_1 \\ \exp(i\delta_1)\sin\theta_1 \end{bmatrix},$$
$$A_2 = |A_2|\begin{bmatrix} \cos\theta_2 \\ \exp(i\delta_2)\sin\theta_2 \end{bmatrix}$$

requires two conditions to be simultaneously satisfied: $\delta_1 + \delta_2 = 0$ and $\theta_1 + \theta_2 = 90°$. There is a continuum of solutions to these conditions corresponding to pump beams with opposite handed elliptical polarization states, however, there are two special cases that maximize the

TABLE I. Some examples of the four-wave mixing transformation matrix M for different pump polarization states.

Pump polarization states		Transformation matrix M
Copolarized linear along $\hat{\mathbf{x}}$	$\mathbf{A}_1 = \mathbf{A}_2 = \begin{bmatrix} 1 \\ 0 \end{bmatrix}$	$2\begin{bmatrix} 1 & 0 \\ 0 & 0 \end{bmatrix}$
Orthogonal linear along axes $\mathbf{x}$ and $\mathbf{y}$	$\mathbf{A}_1 = \begin{bmatrix} 1 \\ 0 \end{bmatrix}$ $\mathbf{A}_2 = \begin{bmatrix} 0 \\ 1 \end{bmatrix}$	$\begin{bmatrix} 0 & 0 \\ 0 & 0 \end{bmatrix}$
Orthogonal circular	$\mathbf{A}_1 = \frac{1}{\sqrt{2}}\begin{bmatrix} 1 \\ i \end{bmatrix}$ $\mathbf{A}_2 = \frac{1}{\sqrt{2}}\begin{bmatrix} 1 \\ -i \end{bmatrix}$	$\begin{bmatrix} 1 & 0 \\ 0 & 1 \end{bmatrix}$
Copolarized linear 45° to x	$\mathbf{A}_1 = \mathbf{A}_2 = \frac{1}{\sqrt{2}}\begin{bmatrix} 1 \\ 1 \end{bmatrix}$	$\begin{bmatrix} 1 & 0 \\ 0 & 1 \end{bmatrix}$
Orthogonal linear ±45° to x	$\mathbf{A}_1 = \frac{1}{\sqrt{2}}\begin{bmatrix} 1 \\ 1 \end{bmatrix}$ $\mathbf{A}_2 = \frac{1}{\sqrt{2}}\begin{bmatrix} 1 \\ -1 \end{bmatrix}$	$\begin{bmatrix} 1 & 0 \\ 0 & -1 \end{bmatrix}$

products of $A_{1x}A_{2x}$ and $A_{1y}A_{2y}$, and therefore maximize the reflectivity. These correspond to $\theta_1 = \theta_2 = 45°$ and either $\delta_1 = -\frac{\pi}{2}, \delta_2 = \frac{\pi}{2}$ (orthogonal circular polarizations) or $\delta_1 = \delta_2 = 0$ (parallel linear polarizations at $\theta = 45°$).

To test the above theoretical prediction, an experimental arrangement to perform FWM in Cr:YAG was set up as shown in Fig. 1. The crystal sample of Cr:YAG, which was supplied by Union Carbide, had a diameter of 9 mm and 4.5 mm thickness, with the propagation directions of the beams along the [100] crystallographic axis and the [010] and [001] axes in the transverse x-y plane. In this work, polarization angles θ of linear polarized light are denoted relative to the x ([010]) axis. The optical beams in this experiment were supplied by a Q-switched Nd:YAG laser (1.064 μm) with pulse duration 16 ns (FWHM) and in a TEM_{00} mode. As noted by other authors the small-signal crystal transmission of our crystal sample ($T_0 = 0.42$) was found to be independent of polarization angle θ, corresponding to equal number of Cr species associated with the two crystallographic axes [010] and [001].

For the demonstration of VPC, the pump beams were given orthogonal circular polarizations by their passage through separate quarter-wave retardation plates. The probe beam was passed through a Glan-air polarizer whose transmission axis was aligned parallel to the x-crystal axis. The polarization of the probe beam was then rotated to an angle θ by passage through a suitably orientated half-wave retardation plate. Figure 2(a) shows the temporal profile of the conjugate beam monitored after it had passed back through the half-wave plate and Glan-air polarizer. There was no rejected polarization component observed from the polarizer. It is seen that the conjugate return is independent of the incident polarization angle of the probe beam and is consistent with the property of VPC. A similar result is obtained if the probe beam passed through a quarter-wave plate. It is noted that the pump beams in the above experiments were at a saturating fluence and cannot be considered weak.

We also conducted the same experiment but with a strongly saturating probe fluence ($U = 5.2U_{\mathrm{sat}}$) and the results are shown in Fig. 2(b). It is seen that the conjugate return through the polarizer is no longer independent of the polarization state and that VPC must be incomplete. Finally, we also tested the ability to produce VPC with parallel linear polarized pump beams at 45° to the crystal axes. We found the same results as for the case of orthogonally circular polarized pump beams, and observed VPC with constant conjugate intensity and no rejected component from the analyzing polarizer for both the case when the (weak) probe beam passed through a half-wave plate or through a quarter-wave plate.

The FWM results with a weak probe and either orthogonally polarized circular pump beams or parallel linear polarization pump beams at 45° to the crystal axes demonstrate the property of VPC. In these cases the effects of the wave plate (half-wave or quarter-wave retarder) are canceled on double passage with a phase conjugate reflection. This is in accordance with the theory in this paper and provides further validation for the model of the polarization dependence of the Cr:YAG absorbing species.

It is also noted, however, that in order to achieve the highest reflectivity we used pump beams at about twice the saturation level, while our theory was for the case of weak saturation. It is possible to discern qualitatively the effects of the strong pumps without a full analysis. Under saturating pump conditions, the pumps and probe will not experience small-signal exponential absorption, so that the conjugate reflectivity predicted by Eq. (5) will be an overestimate. However, since the circularly polarized pump beams have x and y components that are equal in magnitude [$|A_{ix}| = |A_{iy}|$ $(i = 1, 2)$], both crystal axes will be equally saturated and the form of transfer matrix M will still remain proportional to the identity matrix but

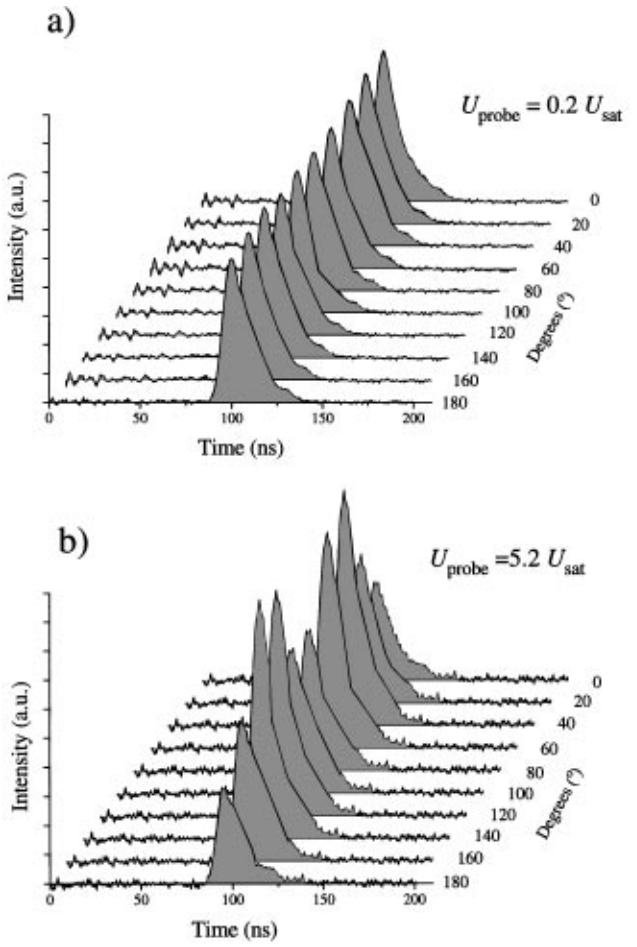

FIG. 2. Temporal profiles of the FWM conjugate beam having returned through the wave plate and polarizer for different polarization angles of the probe beam $\mathbf{E}_3$ incident onto the crystal and where the probe beam has (a) a weak fluence $0.2U_{sat}$ and (b) a strong fluence $5.2U_{sat}$. The counterpropagating pump beams have orthogonal circular polarizations.

with a lower magnitude of diagonal matrix coefficients compared to the weak-saturation prediction [Eq. (4e)].

When the probe also becomes strong this symmetry is expected to be broken, since generally $|A_{3x}| \neq |A_{3y}|$ and $\mathbf{A}_3$ will contribute to different degrees of saturation along the two axes. Since the reflectivity of FWM in a saturable medium is known to be a monotonically decreasing function of the probe intensity [1], this will result in a lower reflectivity seen by the stronger probe component. This must necessarily lead to incomplete depolarization compensation in proportion to the difference in the reflection coefficients of A_{3x} and A_{3y}. This effect is manifest mathematically by the matrix components becoming asymmetric. Incomplete VPC is shown in the strong probe case of Fig. 2(b) in which the VPC component is displayed as a function of angle θ of probe polarization relative to the x axis. Two special cases of angle θ are noted in which cancellation of the effect of the wave plate still occurs; i.e., there is no rejected component from the analyzing polarizer. One is when $\theta = 0°$ or 90°, in which case A_{1y} or A_{1x} is zero and the asymmetry in the two matrix components is unimportant. The other special case occurs when $\theta = 45°$ and $A_{3x} = A_{3y}$, and the components of the matrix elements of Eq. (4e) are equally saturated by the equal probe components. The reason that the VPC return is higher at $\theta = 45°$ compared to $\theta = 0°$, as seen in Fig. 2(b), is due to the higher overall reflectivity compared to $\theta = 0°$, since the strongly saturating probe is split into two equal components leading to lower saturation of each crystallographic axial component and hence to a higher overall reflectivity.

In conclusion, we have developed a model of four-wave mixing in a saturable medium whose saturating species are polarization dependent and lie along orthogonal crystallographic axes as is observed in the solid-state saturable absorber Cr:YAG. As a result, wave mixing of the x and y components of the interacting fields are predicted to occur independently with no cross coupling. This leads to unique pump polarization realizations that can lead to vector phase conjugation of an arbitrary polarization state of a probe beam. We have verified these predictions by four-wave mixing experiments in Cr:YAG at 1.064 μm. We have shown that vector phase conjugation is generally incomplete, however, when the probe beam becomes sufficiently saturating in its own right due to an asymmetry in the reflectivity of the polarization components of the probe beam.

This work was supported by Engineering and Physical Science Research Council (EPSRC) Grant No. GR/K 19501. One of the authors (S. C.-L.) acknowledges support from CONACyT, Mexico.

*Electronic address: m.damzen@ic.ac.uk

[1] R. P. M. Green, G. J. Crofts, and M. J. Damzen, Opt. Commun. **102**, 288 (1993).
[2] A. Brignon, J. Raffy, and J. P. Huignard, Opt. Lett. **19**, 865 (1994).
[3] R. G. Caro and M. C. Gower, IEEE J. Quantum Electron. **18**, 1376 (1982).
[4] G. J. Crofts, R. P. M. Green, and M. J. Damzen, Opt. Lett. **17**, 920 (1992).
[5] I. V. Klimov, M. Yu. Nikol'skii, V. B. Tsvetkov, and I. A. Shcherbakov, Sov. J. Quantum Electron. **22**, 603 (1992).
[6] K. Spairosu, W. Chen, R. Stultz, M. Birnbaum, and A. V. Shestakov, Opt. Lett. **18**, 814 (1993).
[7] H. J. Eichler, A. Haase, M. R. Kokta, and R. Menzel, Appl. Phys. **58**, 409 (1994).
[8] H. Eilers, W. M. Dennis, W. M. Yen, S. Kuck, K. Peterman, G. Huber, and W. Jia, IEEE J. Quantum Electron. **29**, 2508 (1993).
[9] N. G. Basov, V. F. Efimkov, I. G. Zubarev, A. V. Kotov, S. I. Mikhailov, and M. G. Smirnov, JETP Lett. **28**, 197 (1978).
[10] M. Ducloy and D. Bloch, Phys. Rev. A **30**, 3107 (1984).
[11] G. Martin, L. K. Lam, and R. W. Hellwarth, Opt. Lett. **5**, 185 (1980).
[12] R. W. Boyd, *Nonlinear Optics* (Academic Press, Boston, 1992).
[13] J. C. Diels, I. C. McMicheal, and H. Vanherzeele, IEEE J. Quantum Electron. **20**, 630 (1984).
[14] W. P. Brown, J. Opt. Soc. Am. **73**, 629 (1983).